Adaptive Estimation of Measurement Bias in Six Degree of Freedom Inertial Measurement Units: Theory and Preliminary Simulation Evaluation

Andrew R. Spielvogel and Louis L. Whitcomb

***Abstract*— Six-degree of freedom (DOF) inertial measurement units (IMUs) are widely used for attitude estimation. However, such systems' accuracy is limited by the accuracy of calibration of bias, scale factors, and non-orthogonality of sensor measurements. This paper reports a stable adaptive estimator of measurement bias in six-DOF IMUs and preliminary simulation results employing a commercially available IMU comprising a 3-axis fiber optic gyroscope (FOG) with a 3-axis micro-electro-mechanical systems (MEMS) accelerometer. A stability proof of the adaptive estimator and preliminary numerical simulation results are reported. The simulation results for a rotating IMU configuration are promising, and further experimental evaluation and extension of the algorithm for the case of a translating IMU configuration typically found on moving robotic vehicles are needed.**

I. Introduction

Six-degree of freedom (DOF) inertial measurement units (IMUs) are frequently used in many applications including robotics, vehicle navigation systems, and smart-phones. Six-DOF IMUs are comprised of a 3-axis angular-rate gyroscope and a 3-axis linear accelerometer. Angular-rate gyroscopes measure the angular rotation rate of the instrument, while linear accelerometers measure linear acceleration and are often used to measure the device's local level (roll and pitch) with respect to the Earth's local gravity vector.

In addition, six-DOF IMUs are commonly used in attitude estimation systems (eg. [5], [6], [14], [15], [3], [24], [23]). However, these systems' accuracies are affected by biases, scale factors, and non-orthogonality of their sensor measurements. Thus, calibration of these parameters (angular-rate and linear acceleration sensor biases) of six-DOF IMUs is critical for accurate attitude estimation.

A. Literature Review

Several methods for IMU measurement bias estimation have been reported in recent years. However, majority of this literature focuses on magnetometer bias estimation (eg. [2], [1], [4], [7], [9], [11], [13]). In contrast, the present paper addresses angular-rate and linear acceleration sensor bias identification.

Metni et al. and Pflimlin et al. report nonlinear complementary filters for estimating attitude and gyroscope sensor bias ([16], [17], [19]). While these estimators identify angular-rate sensor bias, they do not address linear acceleration sensor bias.

We gratefully acknowledge the support of the National Science Foundation under NSF award OCE-1435818. The authors are with the Department of Mechanical Engineering, Johns Hopkins University, Baltimore, MD 21218, USA. Email: {aspielv1,llw}@jhu.edu

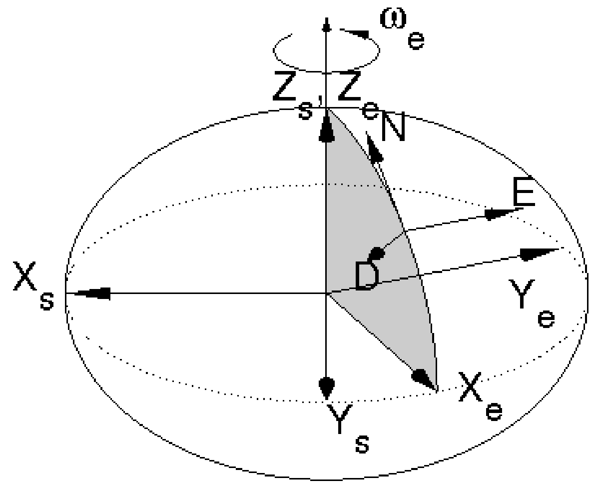

Fig. 1. The star frame (s), Earth frame (e), and NED frame (N). w_e is the Earth's angular velocity with a magnitude of $\sim +15°$/hr.

In [8], George and Sukkarieh report an identifier for accelerometer and gyroscope sensor bias. However, they utilize global positioning system (GPS) which is unsuitable for robotic vehicles operating in GPS-denied environments (eg. submerged vehicles).

Scandaroli et al. and Scandaroli and Morin ([22], [21]) also report a sensor bias estimator for 6-DOF IMUs utilizing computer vision. This method though is dependent on the presence of a vision system, which requires identification markers and a camera system which may not be available for a robotic vehicle (eg. underwater vehicles).

B. Paper's Contribution

The present paper reports (to the best knowledge of the authors) the first stable adaptive algorithm for estimating measurement bias of a dynamic (rotating) six-DOF IMU along with preliminary simulation results of the identifier.

This paper is organized as follows: Section II gives an overview of preliminaries. Section III reports the adaptive measurement bias identifier. Section IV presents numerical simulations. Section V summarizes and concludes.

II. Preliminaries

A. Coordinate Frames

We define the following coordinate frames:

Star Frame: The star frame (s) has its origin at the center of the Earth, with its axes fixed (non-rotating) with respect to the stars, and with its z-axis aligned with the Earth's axis of rotation. For the purpose of this analysis the star frame can be considered an inertial reference frame.

Earth Frame: The Earth Frame (e) has its origin at the center of the Earth, and with its z-axis aligned with the Earth's axis of rotation. The Earth frame rotates with respect to the star frame about their coincident z-axis at the Earth's rotation of $\sim +15°$ per hour.

Instrument Frame: A frame (i) fixed in the IMU instrument.

North-East-Down (NED) Frame: The NED frame (N) has its x-axis pointing North, its y-axis pointing East, its z-axis pointing down, and its origin co-located with that of the instrument frame.

B. Notation and Definitions

For vectors, a leading superscript indicates the frame of reference and a following subscript indicates the signal source, thus ${}^{N}w_m$ is the measured instrument angular velocity in the NED frame and ${}^{i}a_m$ is the measured instrument linear acceleration in the instrument sensor frame.

Definition: The set of 3×3 rotation matrices forms a group, known as the special orthogonal group, SO(3), defined as

$$SO(3) = \{R : R \in \mathbb{R}^{3\times3}, R^T R = I_{3\times3}, \det(R) = 1\}. \quad (1)$$

For rotation matrices a leading superscript and subscript indicates the frames of reference. For example, ${}^{N}_{i}R$ is the rotation from the instrument frame to the NED frame.

The elements of a vector $x \in \mathbb{R}^3$ are defined with the usual subscripts,

$$x = \begin{bmatrix} x_1 \\ x_2 \\ x_3 \end{bmatrix}. \quad (2)$$

Definition: The set of 3×3 skew-symmetric matrices is

$$so(3) = \{S : S \in \mathbb{R}^{3\times3}, S^T = -S\}. \quad (3)$$

Definition: J is a function that maps a 3×1 vector to the corresponding 3×3 skew-symmetric matrix, $J : \mathbb{R}^3 \to so(3)$. For any $k \in \mathbb{R}^3$

$$J(k) = \begin{bmatrix} 0 & -k_3 & k_2 \\ k_3 & 0 & -k_1 \\ -k_2 & k_1 & 0 \end{bmatrix}. \quad (4)$$

We define its inverse $J^{-1} : so(3) \to \mathbb{R}^3$, such that $\forall x \in \mathbb{R}^3$, $J^{-1}(J(x)) = x$.

Definition: The Euclidean vector norm is defined as usual as: $\forall x(t) \in \mathbb{R}^3$

$$\|x(t)\| = \left(x^T(t)x(t)\right)^{1/2}. \quad (5)$$

Definition [10]: A function $V(x)$ is said to be radially unbounded if

$$V(x) \to \infty \text{ as } \|x\| \to \infty. \quad (6)$$

C. Sensor Model

The sensor data is modeled as

$$\begin{aligned} {}^{i}w_m(t) &= {}^{i}w_E(t) + {}^{i}w_v(t) + {}^{i}w_b + {}^{i}\eta_w(t) & (7)\\ {}^{i}a_m(t) &= {}^{i}a_g(t) + {}^{i}a_v(t) + {}^{i}a_b + {}^{i}\eta_a(t) & (8)\\ {}^{i}w_e(t) &= {}^{i}w_E(t) + {}^{i}w_v(t) + {}^{i}w_b & (9)\\ {}^{i}a_e(t) &= {}^{i}a_g(t) + {}^{i}a_v(t) + {}^{i}a_b & (10) \end{aligned}$$

where ${}^{i}w_m(t)$ is the IMU measured angular-rate, ${}^{i}w_e(t)$ is the expected angular-rate, ${}^{i}w_E(t)$ is the true angular velocity due to the rotation of the Earth, ${}^{i}w_v(t)$ is the true angular velocity due to the rotation of the instrument with respect to the NED frame, ${}^{i}w_b$ is the angular velocity sensor bias offset, ${}^{i}\eta_w(t)$ is the zero-mean Gaussian angular velocity sensor noise, ${}^{i}a_m(t)$ is the IMU measured linear acceleration, ${}^{i}a_e(t)$ is the expected linear acceleration, ${}^{i}a_g(t)$ is the true linear acceleration due to gravity and the Earth's rotation, ${}^{i}a_v(t)$ is the instrument's true linear acceleration with respect to Earth, ${}^{i}a_b$ is the linear accelerometer sensor bias, and ${}^{i}\eta_a(t)$ is the zero-mean Gaussian linear accelerometer sensor noise.

For this paper, we assume that the instrument is rotating with respect to the NED frame (${}^{i}a_v(t) = 0$). For robotic vehicles with small peak vehicle accelerations and a zero mean vehicle acceleration over time (eg. underwater vehicles), the acceleration due to gravity is the dominating signal in the acceleration measurement. For this reason, we are ignoring vehicle acceleration (since this formulation is applicable to slowly accelerating vehicles) but are conducting continuing research to extend our algorithm to the accelerating vehicle case. With the zero vehicle acceleration assumption, the sensor data model simplifies to

$$\begin{aligned} {}^{i}w_m(t) &= {}^{i}w_E(t) + {}^{i}w_v(t) + {}^{i}w_b + {}^{i}\eta_w(t) & (11)\\ {}^{i}a_m(t) &= {}^{i}a_g(t) + {}^{i}a_b + {}^{i}\eta_a(t) & (12)\\ {}^{i}w_e(t) &= {}^{i}w_E(t) + {}^{i}w_v(t) + {}^{i}w_b & (13)\\ {}^{i}a_e(t) &= {}^{i}a_g(t) + {}^{i}a_b. & (14) \end{aligned}$$

III. An Adaptive Measurement Bias Identifier

This section reports a novel adaptive bias identifier (6-DOF IMU angular rate and linear acceleration biases) based upon the adaptive estimation of measurement bias in 3-DOF field sensors reported by Troni and Whitcomb in [25].

A. System Model

We consider the system model

$${}^{s}_{N}R(t)\,{}^{N}a_g = {}^{s}_{i}R(t)\left({}^{i}a_e(t) - {}^{i}a_b\right). \quad (15)$$

Differentiating (15), yields,

$$\begin{aligned} {}^{s}_{N}R(t)J\left({}^{N}w_E\right){}^{N}a_g = {}^{s}_{i}R(t)J\left({}^{i}w_e(t) - {}^{i}w_b\right)\left({}^{i}a_e(t) - {}^{i}a_b\right) \\ + {}^{s}_{i}R(t)\,{}^{i}\dot{a}_e(t). \quad (16) \end{aligned}$$

Rearranging terms in (16) yields,

$$\begin{aligned} {}^{i}\dot{a}_e(t) &= {}^{N}_{i}R^T(t)J({}^{N}w_E){}^{N}a_g \\ &\quad - J\left({}^{i}w_e(t) - {}^{i}w_b\right)\left({}^{i}a_e(t) - {}^{i}a_b\right) \\ &= {}^{N}_{i}R^T(t)J\left({}^{N}w_E\right){}^{N}a_g - J\left({}^{i}w_e(t)\right){}^{i}a_e(t) \\ &\quad + J\left({}^{i}w_e(t)\right){}^{i}a_b - J\left({}^{i}a_e(t)\right){}^{i}w_b - {}^{i}z \quad (17) \end{aligned}$$

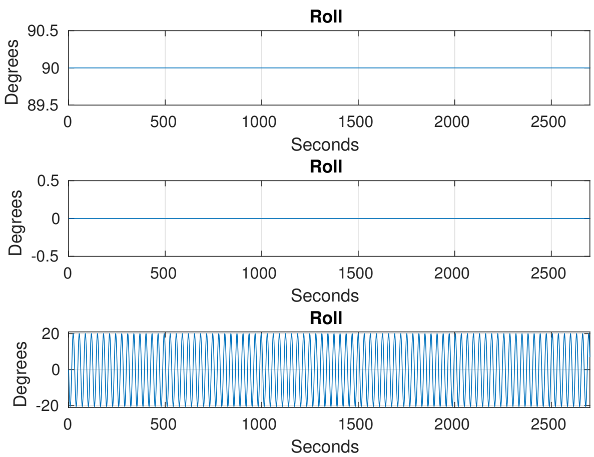

Fig. 2. Simulation dataset attitude.

where ${}^i z$ is the constant ${}^i z = J\left({}^i w_b\right){}^i a_b$.

B. Adaptive Identifier

We consider the identifier system model

$$\begin{aligned} {}^i\dot{\hat{a}}_e &= {}^N_i R^T(t) J\left({}^N w_E\right){}^N a_g - J\left({}^i w_e(t)\right){}^i a_e(t) \\ &\quad + J\left({}^i w_e(t)\right){}^i \hat{a}_b(t) - J\left({}^i a_e(t)\right){}^i \hat{w}_b(t) \\ &\quad - {}^i \hat{z}(t) - k_1 \Delta a(t) \quad (18) \\ {}^i\dot{\hat{w}}_b(t) &= -k_2 J\left({}^i a_e(t)\right)\Delta a(t) \quad (19) \\ {}^i\dot{\hat{a}}_b(t) &= k_3 J\left({}^i w_e(t)\right)\Delta a(t) \quad (20) \\ {}^i\dot{\hat{z}}(t) &= k_4 \Delta a(t) \quad (21) \end{aligned}$$

where the estimation errors are defined as

$$\begin{aligned} \Delta a(t) &= {}^i\hat{a}_e(t) - {}^i a_g(t) \quad (22) \\ \Delta w_b(t) &= {}^i\hat{w}_b(t) - {}^i w_b \quad (23) \\ \Delta a_b(t) &= {}^i\hat{a}_b(t) - {}^i a_b \quad (24) \\ \Delta z(t) &= {}^i\hat{z}(t) - {}^i z. \quad (25) \end{aligned}$$

Note that the attitude (rotation matrix ${}^N_i R(t)$) is needed for the algorithm.

C. Error System

The error system is

$$\begin{aligned} \Delta\dot{a}(t) &= J\left({}^i w_e(t)\right)\Delta a_b(t) - J\left({}^i a_e(t)\right)\Delta w_b(t) \\ &\quad - \Delta z(t) - k_1\Delta a(t) \quad (26) \\ \Delta\dot{w}_b(t) &= -k_2 J\left({}^i a_e(t)\right)\Delta a(t) \quad (27) \\ \Delta\dot{a}_b(t) &= k_3 J\left({}^i w_e(t)\right)\Delta a(t) \quad (28) \\ \Delta\dot{z}(t) &= k_4\Delta a(t). \quad (29) \end{aligned}$$

D. Stability

Consider the Lyapunov candidate function

$$\begin{aligned} V &= \frac{1}{2}\|\Delta a(t)\|^2 + \frac{1}{2k_2}\|\Delta w_b(t)\|^2 \\ &\quad + \frac{1}{2k_3}\|\Delta a_b(t)\|^2 + \frac{1}{2k_4}\|\Delta z(t)\|^2. \quad (30) \end{aligned}$$

Taking the time derivative and substituting in (26) - (29) yields

$$\begin{aligned} \dot{V} &= \Delta a^T(t)\dot{\Delta a}(t) + \frac{1}{k_2}\dot{\Delta w}_b^T(t)\Delta w_b(t) \\ &\quad + \frac{1}{k_3}\dot{\Delta a}_b^T(t)\Delta a_b(t) + \frac{1}{k_4}\dot{\Delta z}^T(t)\Delta z(t) \\ &= -k_1\Delta a^T(t)\Delta a(t) \\ &\quad + \left(-\Delta a^T(t) J\left({}^i a_e(t)\right) + \Delta a^T(t) J\left({}^i a_e(t)\right)\right)\Delta w_b(t) \\ &\quad + \left(\Delta a^T(t) J\left({}^i w_e(t)\right) - \Delta a^T(t) J\left({}^i w_e(t)\right)\right)\Delta a_b(t) \\ &\quad + \left(\Delta a^T(t) - \Delta a^T(t)\right)\Delta z(t) \\ &= -k_1\|\Delta a(t)\|^2. \quad (31) \end{aligned}$$

Since the Lyapunov function is radially unbounded and its time derivative is negative semidefinite, the adaptive identifier is globally stable. In addition, because $\dot{V} = -k_1\|\Delta a(t)\|^2$, the state $\Delta a(t)$ converges asymptotically to zero while the other states, $\Delta w_b(t)$, $\Delta a_b(t)$, and $\Delta z(t)$, are stable. Additional arguments beyond the scope of this paper and persistent excitation (PE) conditions are needed for global asymptotic stability of the adaptive identifier [18], [20].

IV. Numerical Simulations

The performance of the measurement bias adaptive identifier was evaluated with numerical simulations. Section IV-A presents the simulation setup and Section IV-B reports the simulation results.

A. Simulation Setup

- Two numerical simulations (TRUEATT and MAGATT) were implemented using one generated dataset.
- The dataset was sampled at 5kHz for 45 minutes and included sensor noise and sensor bias representative of the KVH 1775 IMU (KVH Industries, Inc., Middletown, RI, USA). Angular velocity sensor and linear accelerometer sensor noises were computed from the IMU manufacturer's specifications [12], as per [26], and sensor biases are chosen to be in line with the KVH datasheet ($\sigma_w = 6.32 \times 10^{-3}$ rads/s, $\sigma_a = 0.0037$ g, ${}^i a_b = \left[1\ 2\ -2\right]^T/10^3$, and ${}^i w_b = \left[-2\ 1\ -1\right]^T/10^5$). These noise and bias characteristics are on par with ones we have observed experimentally while using the 1775 IMU.
- The simulated IMU is mounted to a vehicle. If we define a vehicle frame to be such that the x-axis is pointing forward, the y-axis is pointing starboard, and the z-axis is pointing down, the IMU is mounted such that its coordinate frame's origin is co-aligned with that of the vehicle and rotated by $45°$ around the x-axis (roll).

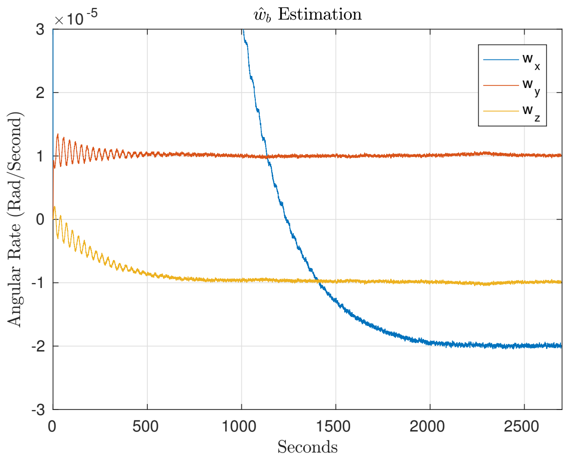

Fig. 3. TRUEATT simulation $\hat{w}_b(t)$ estimate.

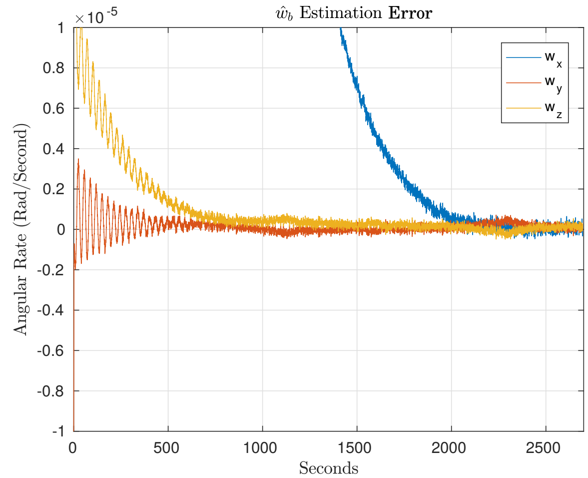

Fig. 4. TRUEATT simulation $\hat{w}_b(t)$ estimates' error.

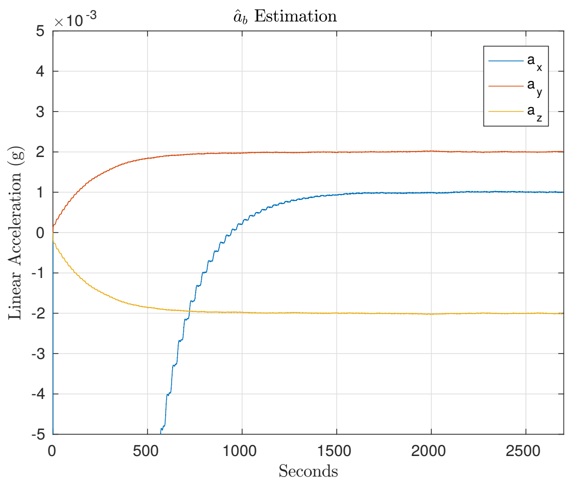

Fig. 5. TRUEATT simulation $\hat{a}_b(t)$ estimate.

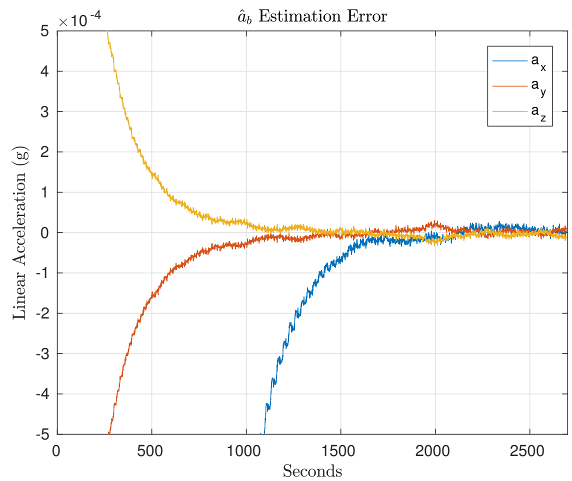

Fig. 6. TRUEATT simulation $\hat{a}_b(t)$ estimates' error.

- During the simulation, the instrument experiences a sinusoidal angular velocity of ${}^{i}w_v(t) = \left[0 - \cos(t/5)/20 - \cos(t/5)/20\right]^T$ which results in the vehicle heading shown Figure 2.

B. Simulations

Both simulations use adaptive identifier gains of $k_1 = 1$, $k_2 = 0.01$, $k_3 = 2$, and $k_4 = 0.000001$.

1) TRUEATT Simulation: The TRUEATT simulation implements the bias adaptive identifier using the true attitude (roll, pitch, heading) for calculating the ${}^{N}_{i}R(t)$ matrix.

2) MAGATT Simulation: The MAGATT implements the bias adaptive identifier using corrupted heading measurements (3° heading bias) for calculating the ${}^{N}_{i}R(t)$ matrix. Accelerometers can be used to find local level (roll and pitch) to within a fraction of a degree, so for this study we focused on the affect of heading error from magnetometers, which is commonly around 3°, on the 6-DOF IMU sensor bias identifier.

C. Results

1) TRUEATT Simulation: The angular rate bias estimation and errors for the TRUEATT simulation are shown in Figures 3 and 4, respectively, while the linear acceleration bias estimation and errors for the TRUEATT simulation are shown in Figures 5 and 6, respectively. The simulation results show that with an accurate knowledge of the ${}^{N}_{i}R(t)$ matrix and the IMU experiencing PE, the bias estimates converge to their true values within the 45 minutes of the simulation.

2) MAGATT Simulation: The angular rate bias estimation and errors for the MAGATT simulation are shown in Figures 7 and 8, respectively, while the linear acceleration bias estimation and errors for the MAGATT simulation are shown in Figures 9 and 10, respectively. The simulation results show that with a knowledge of the ${}^{N}_{i}R(t)$ matrix and the IMU experiencing PE, the linear acceleration bias estimate converges to its true values within the 45 minutes of the simulation, while the angular rate bias estimate converges to a value close to the true sensor bias but with a small offset

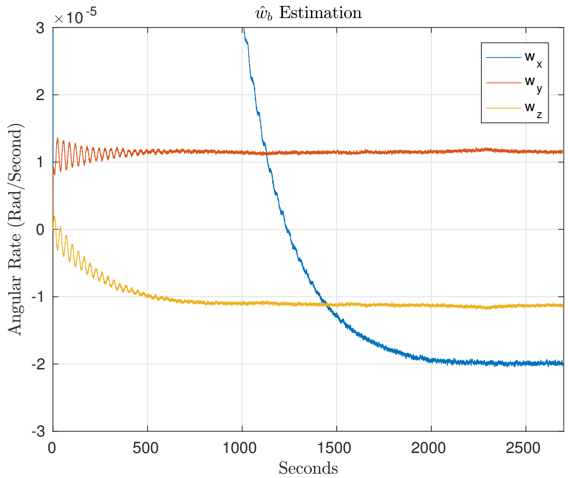

Fig. 7. MAGATT simulation $\hat{w}_b(t)$ estimate.

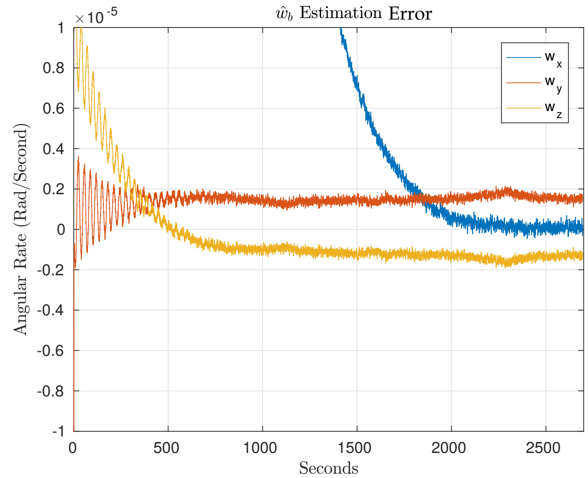

Fig. 8. MAGATT simulation $\hat{w}_b(t)$ estimates' error.

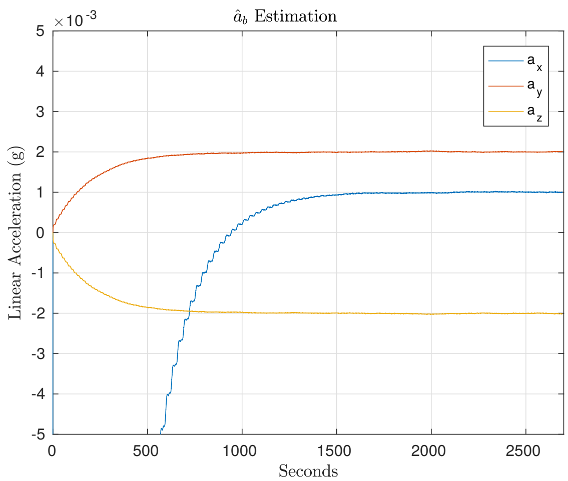

Fig. 9. MAGATT simulation $\hat{a}_b(t)$ estimate.

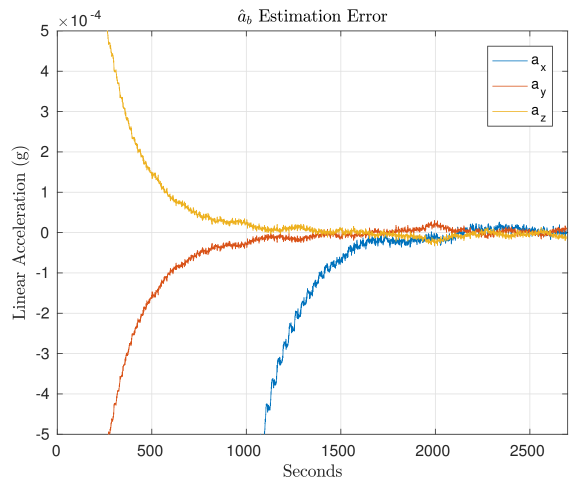

Fig. 10. MAGATT simulation $\hat{a}_b(t)$ estimates' error.

due to the inaccurate heading measurement (3° error).

V. Conclusion

This paper reports a novel stable adaptive 6-DOF IMU measurement bias estimator and preliminary simulation evaluations based on the measurement noise model of the commercially available KVH 1775 IMU data-sheet. The simulation results of a rotating system employing a fiber optic gyroscope (FOG) IMU indicates that algorithm can successfully estimate measurement bias if the attitude (roll, pitch, heading) is known to create the ${}_i^N R(t)$ matrix. Overall, these data suggest the convergence of the adaptive identifier's bias estimates to their true values for the case of a persistently rotating IMU and knowledge of the instruments attitude.

In future research, we will experimentally evaluate the adaptive identifier and address the general use-case of the simultaneously rotating and translating instrument configuration.

References

[1] R. Alonso and M. D. Shuster. Complete linear attitude-independent magnetometer calibration. *Journal of the Astronautical Sciences*, 50(4):477–490, 2002.

[2] R. Alonso and M. D. Shuster. Twostep: A fast robust algorithm for attitude-independent magnetometer-bias determination. *Journal of the Astronautical Sciences*, 50(4):433–452, 2002.

[3] R. Costanzi, F. Fanelli, N. Monni, A. Ridolfi, and B. Allotta. An attitude estimation algorithm for mobile robots under unknown magnetic disturbances. *IEEE/ASME Transactions on Mechatronics*, 21(4):1900–1911, Aug 2016.

[4] J. L. Crassidis, K.-L. Lai, and R. R. Harman. Real-time attitude-independent three-axis magnetometer calibration. *Journal of Guidance, Control, and Dynamics*, 28(1):115–120, 2005.

[5] J. L. Crassidis, F. L. Markley, and Y. Cheng. Survey of nonlinear attitude estimation methods. *Journal of guidance, control, and dynamics*, 30(1):12–28, 2007.

[6] M. Euston, P. Coote, R. Mahony, J. Kim, and T. Hamel. A complementary filter for attitude estimation of a fixed-wing UAV. In *2008 IEEE/RSJ International Conference on Intelligent Robots and Systems*, pages 340–345, Sept 2008.

[7] B. Gambhir. Determination of magnetometer biases using module residg. *Computer Sciences Corporation, Report*, (3000-32700):01, 1975.

[8] M. George and S. Sukkarieh. Tightly coupled INS/GPS with bias estimation for UAV applications. In *Proceedings of Australiasian Conference on Robotics and Automation (ACRA)*, 2005.

[9] P. Guo, H. Qiu, Y. Yang, and Z. Ren. The soft iron and hard iron calibration method using extended Kalman filter for attitude and heading reference system. In *Position, Location and Navigation Symposium, 2008 IEEE/ION*, pages 1167–1174. IEEE, 2008.

[10] H. K. Khalil. *Noninear Systems*. Prentice-Hall, New Jersey, 1996.

[11] M. Kok, J. D. Hol, T. B. Schön, F. Gustafsson, and H. Luinge. Calibration of a magnetometer in combination with inertial sensors. In *Information Fusion (FUSION), 2012 15th International Conference on*, pages 787–793. IEEE, 2012.

[12] KVH Industries, Inc., Middletown, RI, USA. The KVH Web Site http://www.kvh.com and KVH 1775 IMU specifications sheet http://www.kvh.com/ViewAttachment.aspx?guidID=DFB3BCDF-CFA1-422D-837A-92F4F68D9BE5, 2015.

[13] X. Li and Z. Li. A new calibration method for tri-axial field sensors in strap-down navigation systems. *Measurement Science and technology*, 23(10):105105, 2012.

[14] R. Mahony, T. Hamel, and J. M. Pflimlin. Complementary filter design on the special orthogonal group SO(3). In *Proceedings of the 44th IEEE Conference on Decision and Control*, pages 1477–1484, Dec 2005.

[15] R. Mahony, T. Hamel, and J. M. Pflimlin. Nonlinear complementary filters on the special orthogonal group. *IEEE Transactions on Automatic Control*, 53(5):1203–1218, June 2008.

[16] N. Metni, J. M. Pflimlin, T. Hamel, and P. Soueres. Attitude and gyro bias estimation for a flying UAV. In *2005 IEEE/RSJ International Conference on Intelligent Robots and Systems*, pages 1114–1120, Aug 2005.

[17] N. Metni, J.-M. Pflimlin, T. Hamel, and P. Soures. Attitude and gyro bias estimation for a VTOL UAV. *Control Engineering Practice*, 14(12):1511 – 1520, 2006.

[18] K. S. Narendra and A. M. Annaswamy. *Stable adaptive systems*. Courier Corporation, 2012.

[19] J. M. Pflimlin, T. Hamel, and P. Soures. Nonlinear attitude and gyroscope's bias estimation for a VTOL UAV. *International Journal of Systems Science*, 38(3):197–210, 2007.

[20] S. Sastry and M. Bodson. *Adaptive control: stability, convergence and robustness*. Courier Corporation, 2011.

[21] G. G. Scandaroli and P. Morin. Nonlinear filter design for pose and IMU bias estimation. In *2011 IEEE International Conference on Robotics and Automation*, pages 4524–4530, May 2011.

[22] G. G. Scandaroli, P. Morin, and G. Silveira. A nonlinear observer approach for concurrent estimation of pose, IMU bias and camera-to-IMU rotation. In *2011 IEEE/RSJ International Conference on Intelligent Robots and Systems*, pages 3335–3341, Sept 2011.

[23] A. R. Spielvogel and L. L. Whitcomb. Preliminary results with a low-cost fiber-optic gyrocompass system. In *OCEANS 2015 - MTS/IEEE Washington*, pages 1–5, Oct 2015.

[24] A. R. Spielvogel and L. L. Whitcomb. A Stable Adaptive Estimator on SO(3) for True-North Seeking Gyrocompass Systems: Theory and Preliminary Simulation Evaluation. In *Proceedings of the 2017 IEEE International Conference on Robotics and Automation*, May 2017.

[25] G. Troni and L. L. Whitcomb. Adaptive estimation of measurement bias in three-dimensional field sensors with angular rate sensors: Theory and comparative experimental evaluation. In *Robotics: Science and Systems*, 2013.

[26] Woodman, Oliver J. An introduction to inertial navigation. Technical report, University of Cambridge, Cambridge, UK, 2007.